

Method to obtain neuromorphic reservoir networks from images of in vitro cortical networks

Gustavo Borges Moreno e Mello
Dept. of Mech., Elec. and Chem. Engineering
Oslo Metropolitan University
Oslo, Norway
gustavo.mello@oslomet.no

Sidney Pontes-Filho
Dept. of Information Technology
Oslo Metropolitan University
Oslo, Norway
sidney@oslomet.no

Ola Huse Ramstad
Dept. of Neuromedicine and Movement Science
Norwegian University of Science and Technology
Trondheim, Norway
ola.h.ramstad@ntnu.no

Ioanna Sandvig
Dept. of Neuromedicine and Movement Science
Norwegian University of Science and Technology
Trondheim, Norway
ioanna.sandvig@ntnu.no

Vibeke Devold Valderhaug
Dept. of Neuromedicine and Movement Science
Norwegian University of Science and Technology
Trondheim, Norway
vibeke.d.valderhaug@ntnu.no

Evi Zouganeli
Dept. of Mech., Elec. and Chem. Engineering
Oslo Metropolitan University
Oslo, Norway
evi.zouganeli@oslomet.no

Axel Sandvig
Dept. of Neuromedicine and Movement Science
Norwegian University of Science and Technology
Trondheim, Norway
axel.sandvig@ntnu.no

Stefano Nichele
Dept. of Information Technology
Oslo Metropolitan University
Oslo, Norway
stefano.nichele@oslomet.no

Abstract—In the brain, the structure of a network of neurons defines how these neurons implement the computations that underlie the mind and the behavior of animals and humans. Provided that we can describe the network of neurons as a graph, we can employ methods from graph theory to investigate its structure or use cellular automata to mathematically assess its function. Additionally, these graphs can provide biologically plausible designs for networks, which can be integrated as reservoirs to support computing. Although, software for the analysis of graphs and cellular automata are widely available. Graph extraction from the image of networks of brain cells remains difficult. Nervous tissue is heterogeneous, and differences in anatomy may reflect relevant differences in function. Here we introduce a deep learning based toolbox to extract graphs from images of brain tissue. This toolbox provides an easy-to-use framework allowing system neuroscientists to generate graphs based on images of brain tissue by combining methods from image processing, deep learning, and graph theory. The goals are to simplify the training and usage of deep learning methods for computer vision and facilitate its integration into graph extraction pipelines. In this way, the toolbox provides an alternative to the required laborious manual process of tracing, sorting and classifying. We expect to democratize the machine learning methods to a wider community of users beyond the computer vision experts and improve the time-efficiency of graph extraction from large brain image datasets, which may lead to further understanding of the human mind.

Index Terms—neural network, deep learning, graph, reservoir computing, segmentation, cellular automata, in-painting

I. INTRODUCTION

One of the goals of systems neuroscience is to obtain a mechanistic model that describes and explains how networks of neurons in the brain implements perception, thought, and behavior. Because structure implements function in biology, an unavoidable step towards these mechanistic models is to describe the structural connectivity of the network of neurons in the brain. Once a connectivity map (i.e., the description of the network) from a network of neurons is obtained, the it can be described as a graph or a cellular automaton. This description may then be used as constraint to leverage methods from graph theory [1] to further analyze the network structure, or its functional complexity [2], which could ultimately contribute in three ways. First, by moving further the understanding on how to use biological substrates for computing [3], [4]. Second, by improving computing methods in AI by supplying biologically derived network structures that can be used as reservoir networks [5]. Finally, by offering an mathematical abstraction of the biological system that can be used to compare neural networks with endogenous or induced

pathology with the healthy ones [6], providing ground for medical advancements.

Nonetheless, obtaining these matrices of structural connections between neural nodes is a challenging and cumbersome endeavour. Especially from microscopy images (see Fig. 1). Although some methods have been recently developed to automatize the process, they still rely on basic image processing steps that demand substantial time to find suitable parameters and curate the results [7]. Furthermore, these automatic methods are not very robust, and as an effect, the gold standard approach still is to trace these connections manually.

Unlike other biological substrates from which networks can be extracted, the brain is constituted of billions of neurons with diversified morphology, and a few orders of magnitude higher number of connections (i.e., synapses) [8]. This additional complexity implies that different nodes in a graph network should have different properties and represent different cell types or structures in the brain. Because this structural information is critical to understand the brain, it is of utmost importance that automatic tools take them into account. To the best of our knowledge, such methods are not currently available.

Furthermore, experimental constraints (e.g., multi-electrode arrays, patching pipettes) frequently obstruct the view of part of the image (black lines in Fig. 1), consequently preventing the connection of nodes that otherwise would be linked. Although these gaps can be easily handled by human intervention (i.e., by estimating the edges that connect two nodes), no simple image processing method can properly handle this problem as the data in the obstructed area is missing. To cope with this problem, one must be able to reconstruct the missing data by inferring how it would look like based on the surrounding area and what is typically known about the morphology.

Modern machine learning techniques that leverage the power of convolutional neural networks (ConvNets) may be used to automatize many of the steps mentioned earlier. In-painting algorithms can be used to estimate missing data caused by image obstruction, object detection algorithms can be employed to locate and classify diverse structures in the brain, and unsupervised segmentation algorithms can be leveraged to extract skeletonized versions of the image, just to name a few. This would allow for a comprehensive graph extraction from image in neuroscience settings. The challenge regarding employing ConvNets is that due to its novelty and complexity, deep learning methods are not widely available to non-specialists in computer vision. Additionally, most of these methods require training, which by itself is generally poorly documented, preventing non-expert in computer vision from experimenting and benefiting from ConvNets in their neuroscience research.

Motivated by the foregoing shortcomings, we present a deep learning based toolbox to extract graphs from images of in vitro cortical networks. This toolbox is a framework constituted by an extensible library of methods that can be integrated into a computer vision pipeline. The library is based

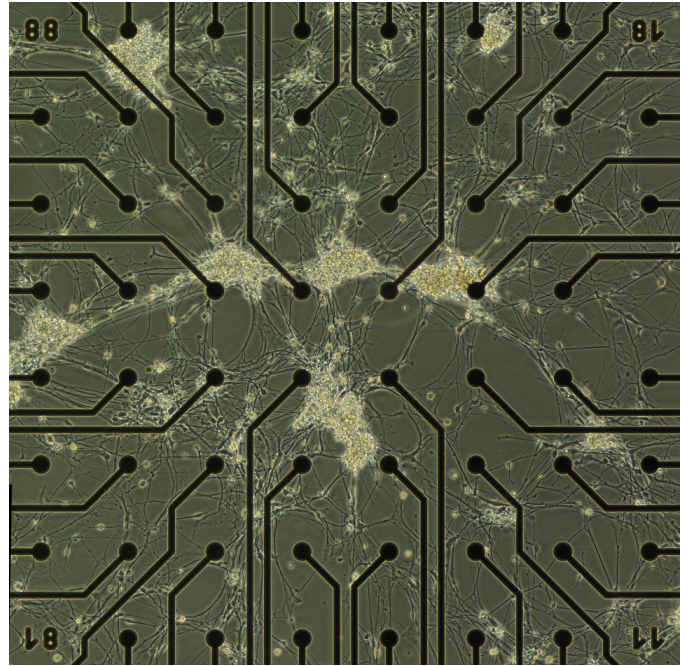


Fig. 1. Raw image example as acquired from the microscope. The black lines ending in circle are "blind-spots" created by the multi-electrode array.

on a combination of standard image processing algorithms available in OpenCV [9] and SKimage [10], and deep learning based methods for object detection, image/line segmentation, in-painting and style transfer implemented in Pytorch [11]. Additionally, the toolbox has a graphical user interface (GUI) that simplifies the steps of assembling the graph extraction pipeline, which includes the training of the supervised machine learning algorithms.

The main contribution of this paper is to make available deep learning based methods for computer vision to the neuroscience community through a reusable, flexible and scalable tool. Through this toolbox, we hope to make deep learning methods more widely accessible to neuroscientists.

II. IMAGE ACQUISITION

The images were prepared as follows: human cortical neural networks were differentiated and matured from iPSC-derived NSCs (ax0019, Axol bioscience). Each multi-electrode array (MEA) was briefly sterilized using ethanol, washed with water, UV-treated over-night, and hydrophilized by application of foetal bovine serum for 30-60 minutes at room temperature. The surface was subsequently double-coated using poly-L-ornithine (0,01%) and laminin. The appropriate neuronal cell culture media were heated to 37°C and used to create a single-cell suspension, from which 100.000 cells were seeded directly onto the electrode area of each MEA in a dropwise manner. For some cultures, a feeder-layer of astrocytes (5000 per MEA) was first established, upon which 50 000 neuronal cells were seeded onto. The MEA neuronal cultures were kept in a standard humidified air incubator (5% CO₂, 20% O₂, 37°C), and 50% of the media were changed every 2-3 days.

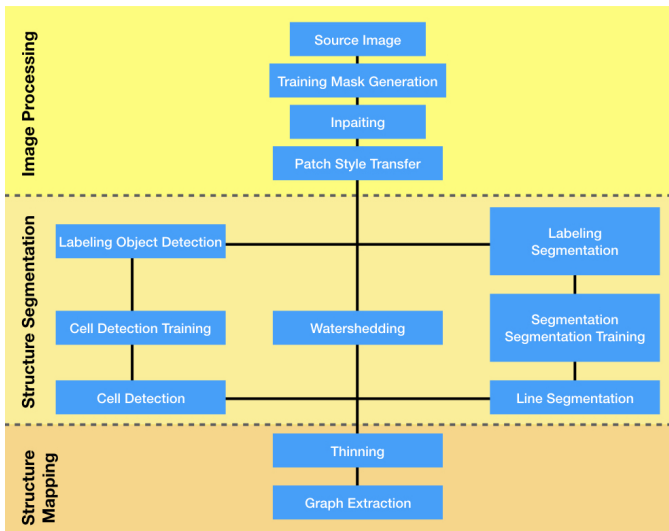


Fig. 2. Graph extraction pipeline.

Phase contrast images were acquired at various stages of neuronal differentiation and maturation on the MEAs using the laboratory light microscope Carl Zeiss Axiovert 25 with 5 and 10X objectives.

III. THE PIPELINE

The kernel of the toolbox is the graph extraction pipeline (Fig. 2). It enables visualization, correction and analysis of the structures depicted in the input image. This pipeline consists of an ordered sequence of methods, which will output a graph representation of the network from the input image. Additionally, some of the steps of the pipeline require preparation (i.e., training) in case of different acquisition setup. The obtained graph provides weights, edge lengths and node type, which should reflect anatomical structure.

The default pipeline combines algorithms in three major categories that correspond to the sequential series of stages in the pipeline: image processing, structure segmentation, and structure mapping, which ultimately outputs a graph that can be further pruned. What follows is a high-level description of the stages.

A. Image processing

Image pre-processing involves doing image transformations that allows the subsequent algorithms to perform more robustly. Our method has a set of ready-to-use algorithms that may be employed interchangeably to compose the image processing steps. Most of them are standard image transformations like color space change and filtering (including sharpening and blurring), widely available through OpenCV and SKimage libraries. Additionally, deep learning based algorithms were included, namely: style transfer [12] and inpainting [13]. These two methods rely on VGG16 networks pre-trained on ImageNet dataset [14], but may be adjusted to leverage [15] other networks such as inception, which

allegedly will improve their accuracy. Because these algorithms must be further fine-tuned to properly work with the dataset from the experiments (see training), training steps were included in the pipeline to make the process intuitive. The reason why in-painting (Fig. 3D) and style transfer (Fig. 3E) were included in the pipeline is because they enable to cope with missing data. This data loss is caused by obstruction of the field of view during experiments. These obstructions are common in histological experiments as often electrodes and pipettes (which are optically obstructive) are used to measure physiological parameter from cells (see black marks in Fig. 1). Additionally style transfer enable reducing problems caused by differences in imaging settings, which tend to affect segmentation, detection and classification algorithms. Finally, to facilitate and speed up the graph extraction, the image is subdivided in squared tiles of 256x256 pixel. The entire pipeline is performed on each individual tile. The output of this step is a image that is free of obstructive artifacts, such as electrodes and pipettes, and properly balanced to match low level features found in the remaining of the dataset.

B. Structure segmentation

In the structure segmentation stage, two things are crucial. First is to build a mask that describes the network of neurites (projection structures of the dendrites), which ultimately will allow to build a connectivity map with edges and nodes. And second, to identify which of the nodes are likely to be morphological relevant structures such as neurons, astrocytes (glial cells) or cluster of neurons, because this information can be used to further prune the network map once it is obtained.

We provide two interchangeable avenues for unsupervised segmentation: Guided watershed [16] and W-Net [17]. We noticed that depending on the characteristics of input image these algorithms perform the best. The main goal of this step is to separate the structures that compose the network from everything else and compose a mask. Additionally, supervised methods can be employed, requiring two additional steps, which is labeling and training as part of the pipeline. Although we tried different methods, binary segmentation was best obtained using the method described in Shvets et al. [18], adapting the AlbuNet-34 to work with images of 256x256 pixels. Thus this method is provided as the standard alternative to unsupervised segmentation.

In order to detect nodes that belong to different cell types, the object detection algorithm, yolov3 (You Only Look Once, version 3.0) [19], was included in the pipeline. This method operates by detecting combinations of spatial features in the image, locating their position and area, and classifying them under a predefined category (namely: astrocytes, neurons and clusters of neurons; see Fig. 3F) with an explicit probability. This algorithm requires training, and substantial amount of data to be trained (see training). The center of these detected areas is used by later steps in the pipeline to discriminate synaptic nodes from cell body nodes.

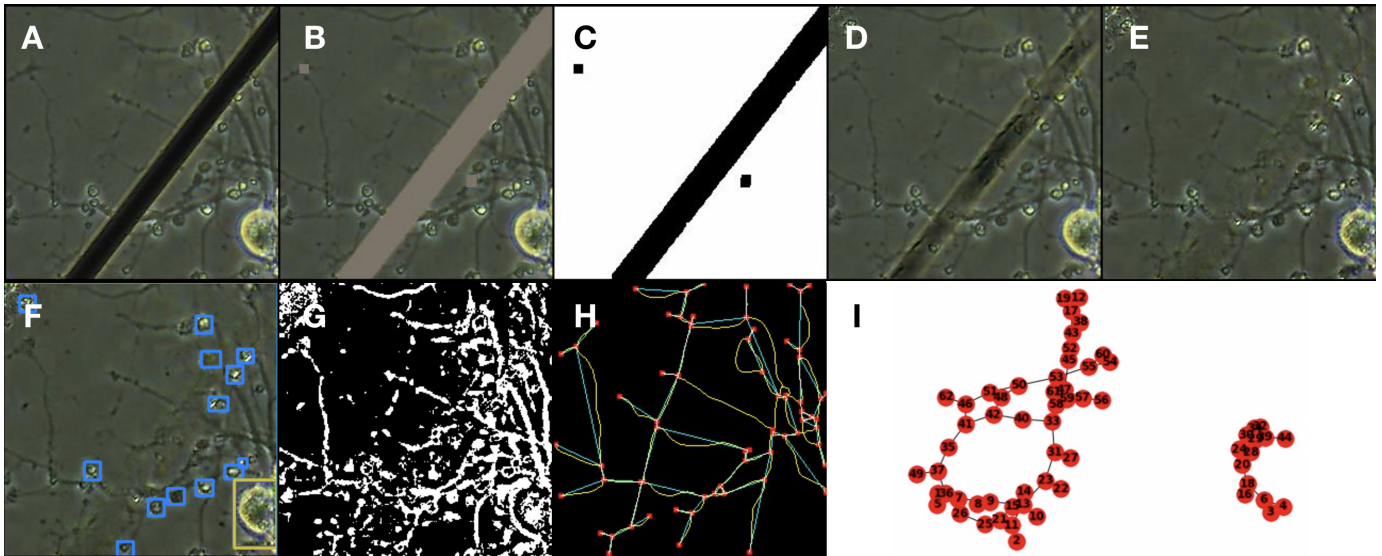


Fig. 3. Graph extraction example. A- 256 x 256 Crop of a raw image as acquired from the microscope. B- Segmentation of the electrode area in grey. C- Mask of the area to be in-painted. D- Intermediate step in the inpainting process. E- End result of the inpainting algorithm. F- Cells identified by type with yolov3, blue boxes are neurons, yellow box is a cluster of cells, astrocytes are omitted. G- Intermediate step of the structure segmentation. H- Graph extraction example, the red represents the nodes, the blue are the edges connecting the nodes and the yellow is the thinned (skeletonized) version of the network identified. I- Graph output describing the network in H.

C. Structure Mapping

Once the previous stages are performed to every patch of the image, the information is used to reconstitute the complete binary mask of the image and proceed with the following steps: Thinning and Graph extraction.

1) *Thinning*: The next step is to skeletonize the mask so no pixel in the mask has two or more neighbor pixels that belongs to the mask and are neighbor to each other (see Fig. 3H, yellow lines). To do that, we implemented the improved Zhang-Suen Thinning algorithm [20]. This method was chosen because it produced less artifacts in the intersection of lines (blobs and missing pixels).

2) *Graph extraction*: Having obtained the skeletonized image we then detect the positions of nodes and the edges that connect them so we can create a graph. The graph is generated through the NetworkX [21] library. To detect the nodes, we filter the image with series of 3x3 filters. Each filter represent one possible scenario for a node where the center pixel belongs to the filter and one or at least three other neighbors also belong to it and are not neighbors to each other. This guarantees that intersection nodes and end-of-the-line nodes are contemplated, but those points that belong to lines are ignored.

Edges between nodes are detected by the following steps. Firstly, the skeleton is segmented in edges by removing the node pixels from the skeletonized mask, each one of these edges has its own label automatically defined as 1 to the number of available edges. Secondly, these segmented edges are dilated. Thirdly, the edges that overlap with two nodes are added to the graph as a bidirectional edge. Finally, the overlapping segmented edge is removed from the set of

possible edges. The process repeats until no edges are left (see Fig. 3H blue lines).

If the Structure Detection step has been executed successfully, the nodes which are closest to the center of the regions of interest generated by the object detection algorithm will acquire the category of the identified object (e.g., neuron, cluster).

This type of representation of the network in graph is analogous to a connectivity estimation, which is highly relevant in neuroscience to infer functionality. Hence the graph extraction method can contribute to connectivity analysis as performed by Maccione et al. [2] and Ullo et al. [22], but without the cumbersome and time-demanding step of extracting the connectivity map manually.

D. Graph pruning

Graph pruning is the procedure of editing the connections in the graph to remove false positives and include false negative nodes and edges. The process has two components: one automatic and one manual. Nodes that are identified as belonging to identified astrocytes are removed, and all the associated edges, because these connections do not translate into possibly functional connections with respect of transmitting information. This process is done automatically without the intervention of the user. As the last step, it is given to the user the opportunity to edit the graph extracted by removing or adding new edges, tracing new edges between them and assigning properties to each node. This is done through graphic interface where the representation of the connectivity map (Fig. 3H) is overlapped with the ground truth image (Fig. 3A).

E. Training

In order to use the methods that depend on supervised learning, the user has to provide first a set of good examples so the algorithm can be properly trained. This process is usually poorly documented and the data format that the algorithm should receive is usually obscure. We make this step explicit, by declaring exactly what should be the data format, and providing a simple interface that the users can use to generate the training data themselves and train the model.

1) *Training in-painting*: To train the in-painting [13] network, we need a set of ground truth images, and a set of masks that would match in shape and size the typical artifact obstructing the original image. To generate this data, we segmented the dark areas of original raw image using a simple threshold. We dilated the segmented areas with a 5x5 circular kernel to include the edges of the artifact areas. We randomly cropped the mask image in images of 256x256 pixels. The images in which 1/4th of the area was occupied by the electrode mask were selected for the mask pool. Each mask was then copied 35 times and rotated cumulatively by 10 degrees until we had 36 versions of the same mask in all orientations.

To extract the ground truth images, we cropped patches of 256x256 pixels from the original image where no pixel in the patch overlapped with the coordinates of a pixel belonging to a mask. To expand the dataset, the selected patches were flipped and rotated 90, 180 and 270 degrees.

2) *Training Semantic Segmentation*: Semantic segmentation using Albunet-34 requires a binary mask of 256x256 pixels (matching the image input size). For each of the images in the training set the user has to paint the mask with an inbuilt interface implemented with tkinter. The dataset is amplified by adding horizontal and vertical flipped version of the input image and matching mask. As training metric we used the variation of the Jaccard Index [18]:

$$I = \frac{1}{n} \sum_{i=1}^n \left(\frac{y_i \hat{y}_i}{y_i + \hat{y}_i - y_i \hat{y}_i} \right) \quad (1)$$

Where I is the metric for intersection over union of binary pixels, y_i is the ground truth binary value of the pixel in the target mask, and \hat{y}_i is the prediction probability associated to the same pixel.

3) *Training object detection*: To train the Yolov3, we defined regions of interests (ROIs) by drawing a bounding boxes from a subset of patches (100 images, randomly picked). This ROIs are constrained by the vertical and horizontal coordinates of its centroid and its height and with as ratios of the original image. Each ROI is labeled as an instance of a class of objects.

In our dataset, we defined three labeled structures: neurons, astrocytes and cluster of neurons. Only neurons and cluster of neurons were relevant for the graph extraction, thus only these two labels are displayed. The labeling of astrocytes was required to prevent falsely detecting astrocytes as neurons. Once training data is available, training follows by pointing

the location of the data in the storage unit and running the training function.

Because the amount of data was limited, the network was pre-trained with the COCO dataset [23] to learn and then fine-tuned and cross-validated using the labeled images. Our implementation of Yolov3 operates by predicting 3 boxes in 2 different scales. Thus, the tensor is $N \times N \times [2*(4+1+3)]$, where 4 is for the 4 bounding box offsets, 1 for objectness prediction, and 3 is for the class predictions. Furthermore we chose 6 clusters in the k-means algorithm to establish our bounding box priors. In our dataset the 6 clusters were (7x9), (15x16), (22x19), (31x32), (55 x 49), (89x91).

The training progress was displayed on every set of epochs, which could be defined by the user, and it could be interrupted at any time. The set of weights with the smaller error was highlighted to facilitate the use of the pipeline.

IV. DISCUSSION

We presented here a deep learning based pipeline to build a graph that represents the connectivity of a network of biological neurons extracted from a microscopy image. This method represents a substantial step forward in developing neuromorphic networks. Because it provides means to explore how biologically developed connections might implement brain-like computing and intelligence.

Many solutions exist to extract network graphs from images, including some generic flexible tools. But these tools assume that the network to be extracted is homogeneous (i.e., all the nodes are equal). This is a major problem in neuroscience because biological neurons form highly heterogeneous networks. In particular, the tools available cannot account for the difference between neurons and synapses as nodes. Additionally, they cannot account for differences between cell types (i.e., neurons vs. glia). This is a major source of error for describing a network. The abundance of false positives can lead to a description that is much bigger and dense, hence increasing the level of complexity which by itself increases the challenge of analysis. Our toolbox circumvents this problem by integrating machine learning methods into an easy to use pipeline to extract graphs from network of neurons. Because the algorithm detects objects by category, further developments may be implemented to extract sub-populations of neurons and include more cell types. One possible avenue is to develop a specific dataset for brain cell-type detection, which is currently unavailable in the best of our knowledge.

A second major challenge in the path of automatizing graph extraction from images of in vitro neural networks is that these images often come with major artifacts (e.g., electrodes, pipettes, objects that obstruct the view). We eliminated these artifacts by combining in-painting techniques and style transfer through deep learning methodologies. Although not perfect, we demonstrate that both techniques can provide qualitatively satisfactory results, allowing to reconstruct a plausible network, despite the artifact. One further point of development could be to apply techniques to improve the resolution, as it

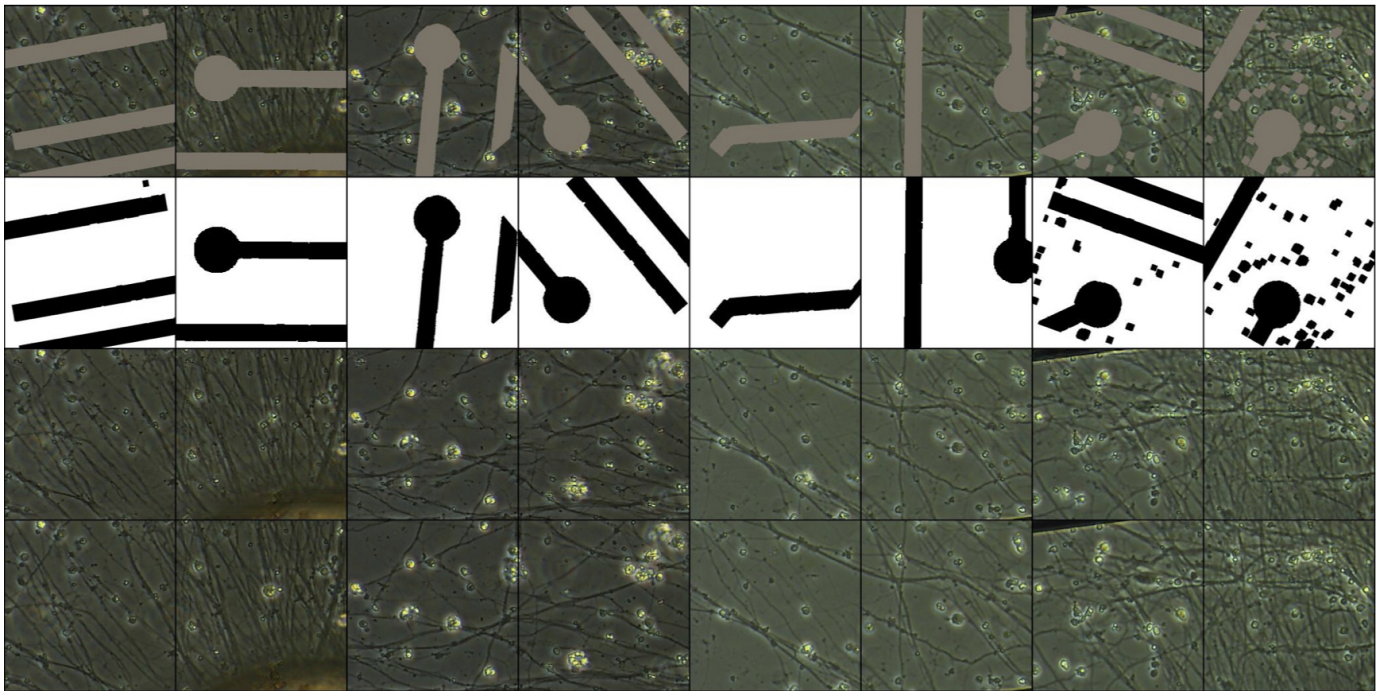


Fig. 4. Inpaint Training. Each column shows inpainting applied to a different patch of image (ground truth is the lowest row) that was free from visual occlusion. Masks (in the second row) were extracted from areas in black occupied by the of the electrodes in other patches, rotated and applied on top of the ground truth to create the input image (first row). The third row shows the output of the inpainting.

may increase the performance of in-painting and style transfer techniques.

We anticipate that this toolbox will enable neuroscientists to extract graphs from network of neurons in a more time-efficient way and consequently contribute in the pursue of the understanding of perception, intelligence and behavior.

ACKNOWLEDGMENT

This work was supported by Norwegian Research Council SOCRATES project (grant number 270961) and received internal support as a lighthouse project in Computer Vision from the Faculty of Technology, Art and Design (TKD) at Oslo Metropolitan University, Norway.

REPOSITORY

Code and example data can be found in the following repository: <https://github.com/gmorenomello/rfbi>

REFERENCES

- [1] M. M. Hassan and G. L. Hogg, "A review of graph theory application to the facilities layout problem," *Omega*, vol. 15, no. 4, pp. 291–300, 1987.
- [2] A. Maccione, M. Garofalo, T. Nieuw, M. Tedesco, L. Berdondini, and S. Martinoia, "Multiscale functional connectivity estimation on low-density neuronal cultures recorded by high-density cmos micro electrode arrays," *Journal of neuroscience methods*, vol. 207, no. 2, pp. 161–171, 2012.
- [3] H. Broersma, J. F. Miller, and S. Nichele, "Computational matter: Evolving computational functions in nanoscale materials," in *Advances in Unconventional Computing*, pp. 397–428, Springer, 2017.
- [4] P. Aaser, M. Knudsen, O. H. Ramstad, R. van de Wijdeven, S. Nichele, I. Sandvig, G. Tufte, U. Stefan Bauer, Ø. Halaas, S. Hendseth, et al., "Towards making a cyborg: A closed-loop reservoir-neuro system," in *Artificial Life Conference Proceedings 14*, pp. 430–437, MIT Press, 2017.
- [5] S. Nichele and A. Molund, "Deep reservoir computing using cellular automata," *arXiv preprint arXiv:1703.02806*, 2017.
- [6] I. Sandvig, I. L. Augestad, A. K. Håberg, and A. Sandvig, "Neuroplasticity in stroke recovery. the role of microglia in engaging and modifying synapses and networks," *European Journal of Neuroscience*, vol. 47, no. 12, pp. 1414–1428, 2018.
- [7] M. Dirnberger, T. Kehl, and A. Neumann, "Nefi: Network extraction from images," *Scientific reports*, vol. 5, p. 15669, 2015.
- [8] E. R. Kandel, J. H. Schwartz, T. M. Jessell, D. of Biochemistry, M. B. T. Jessell, S. Siegelbaum, and A. Hudspeth, *Principles of neural science*, vol. 4. McGraw-hill New York, 2000.
- [9] B. Gary, "Opencv is an open-source, computer-vision library for extracting and processing meaningful data from images.," *Dr Dobbs*, no. 25, pp. 120–126, 2000.
- [10] S. Van der Walt, J. L. Schönberger, J. Nunez-Iglesias, F. Boulogne, J. D. Warner, N. Yager, E. Gouillart, and T. Yu, "scikit-image: image processing in python," *PeerJ*, vol. 2, p. e453, 2014.
- [11] A. Paszke, S. Gross, S. Chintala, G. Chanan, E. Yang, Z. DeVito, Z. Lin, A. Desmaison, L. Antiga, and A. Lerer, "Automatic differentiation in pytorch," *Open review preprint https://openreview.net/pdf?id=BJJrmfCZ*, 2017.
- [12] L. A. Gatys, A. S. Ecker, and M. Bethge, "A neural algorithm of artistic style," *arXiv preprint arXiv:1508.06576*, 2015.
- [13] G. Liu, F. A. Reda, K. J. Shih, T.-C. Wang, A. Tao, and B. Catanzaro, "Image inpainting for irregular holes using partial convolutions," in *Proceedings of the European Conference on Computer Vision (ECCV)*, pp. 85–100, 2018.
- [14] K. Simonyan and A. Zisserman, "Very deep convolutional networks for large-scale image recognition," *arXiv preprint arXiv:1409.1556*, 2014.
- [15] M. Z. Alom, T. H. Aspiras, T. M. Taha, and V. K. Asari, "Skin cancer segmentation and classification with NABLA-N and inception recurrent residual convolutional networks," *CoRR*, vol. abs/1904.11126, 2019.
- [16] V. Osma-Ruiz, J. I. Godino-Llorente, N. Sáenz-Lechón, and P. Gómez-

Vilda, "An improved watershed algorithm based on efficient computation of shortest paths," *Pattern Recognition*, vol. 40, no. 3, pp. 1078–1090, 2007.

- [17] X. Xia and B. Kulis, "W-net: A deep model for fully unsupervised image segmentation," *arXiv preprint arXiv:1711.08506*, 2017.
- [18] A. A. Shvets, V. I. Iglovikov, A. Rakhlin, and A. A. Kalinin, "Angiodysplasia detection and localization using deep convolutional neural networks," in *2018 17th IEEE International Conference on Machine Learning and Applications (ICMLA)*, pp. 612–617, 2018.
- [19] J. Redmon and A. Farhadi, "Yolov3: An incremental improvement," *arXiv preprint arXiv:1804.02767*, 2018.
- [20] W. Chen, L. Sui, Z. Xu, and Y. Lang, "Improved zhang-suen thinning algorithm in binary line drawing applications," in *2012 International Conference on Systems and Informatics (ICSAI2012)*, pp. 1947–1950, IEEE, 2012.
- [21] A. Hagberg, P. Swart, and D. S Chult, "Exploring network structure, dynamics, and function using networkx," tech. rep., Los Alamos National Lab.(LANL), Los Alamos, NM (United States), 2008.
- [22] S. Ullo, T. R. Nieuw, D. Sona, A. Maccione, L. Berdondini, and V. Murino, "Functional connectivity estimation over large networks at cellular resolution based on electrophysiological recordings and structural prior," *Frontiers in Neuroanatomy*, vol. 8, p. 137, 2014.
- [23] T.-Y. Lin, M. Maire, S. Belongie, J. Hays, P. Perona, D. Ramanan, P. Dollár, and C. L. Zitnick, "Microsoft coco: Common objects in context," in *European conference on computer vision*, pp. 740–755, Springer, 2014.